Larbi Ben M'hidi University - Oum El Bouaghi - ALGERIA
Faculty of Sciences and applied Sciences - Ain El Beida
Laboratory of Electronics and New Technologies

Certificate of Attendance

This is to certify that

Lakhdar DJAGHDALI

has attended the 1st International Conference on Electronics, Artificial Intelligence and new technologies, and presented the paper entitled

Torque ripple reduction of induction machine a comparison between two approaches DTC-SVM

Authors:

This conference is organized by Laboratory of Electronics and New Technologies **(LENT)**, with the sponsorship of theThematic Research Agency in Science and Technology **(ATRST).**

The conference Chair
- President of the Conference -
Pr.Mohamed Lashab

Ministry of Higher Education and Scientific Research
THE 1st INTERNATIONAL CONFERENCE ON ELECTRONICS ARTIFICIAL INTELLIGENCE AND NEW TECHNOLOGIES
ICEAINT
Oum El Bouaghi University

December 8-9, 2021.

ID : 65

Thematic Research Agency in Science and Technology – ATRST-

University Larbi ben M'hidi Oum el Bouaghi. Algeria

Laboratory of Electronics and New Technologies –LENT-

THE 1ST INTERNATIONAL CONFERENCE

ON ELECTRONICS, ARTIFICIAL INTELLIGENCE AND NEW TECHNOLOGIES

ICEAINT

November 29-30, 2021

Online presentation is possible

ISBN: 978-9931-9728-1-5

The Electronics and New Technologies Laboratory (LENT) is organizing the first international conference on electronics, artificial intelligence and new technologies (ICEAINT'21), this will be held at the University of Larbi Ben M'hidi, Oum El Bouaghi. The conference will cover all the research activities of the laboratory; moreover, the conference will include different axes of electronics, computer science and new technologies likely to interest all researchers in these fields. The ICEAINT'21 aims to bring together academic researchers and industrial scientists to exchange new ideas, original research results and practical development experiences on all aspects dealing with the different themes of the conference.

Topics

Topic 1	Topic 2	Topic 3
Telecommunications and antennas	**Control, modelling and artificial intelligence**	**Micro and nanoelectronics**
Chairs : **Pr. Mohamed Lashab** and **Dr. Semira Hichem**	Chairs : **Pr. Kheireddine Lamamra** and **Dr. Abderrahim Faycal Megri**	Chairs : **Pr. Souheil Mouetsi** and **Pr. Abdesselam Hocini**
- Wireless communications - Satellite and space communications - Cognitive radio networks - Wireless multimedia networks - Green wireless networks - 4G and 5G communication networks - Optical communication - Wireless network security and privacy - Antennas and wave propagation - LTE, LTE-Advanced, Wifi, and Wimax - Robotics and vision - Signal and image processing.	- Neural network and deep learning - Machine learning - Control of nonlinear systems - Fuzzy intervals and fuzzy systems - Robust control - Fuzzy control and intelligent systems - Adaptive and predictive control - Modeling and simulation - Identification and estimation - Renewable energy systems applications - Smart city - Embedded systems.	- Semiconductor devices - Thin solid films - Circuit theory and applications - Optoelectronics and photonic crystal - Solid-state electronics - Quantum electronics - Nanoelectronics and spintronics - Photovoltaic - Modeling and simulation, synthesis and verification of ICs - Electronic materials science and technology.

Registration fees

Participants : 5000 DA (Presentation) / 10000 DA (All Inclusive)
Students: 3000 DA (Presentation) / 8000 DA (All Inclusive)
Foreigners: 100 € (Presentation) / 200 € (All Inclusive)
~ Registration fees are to be sent or paid at arrival.

Deadlines

Submission deadline: 15 August 2021
Notification of acceptance: 15 September 2021
Camera ready: 30 September 2021
Conference dates: 29 - 30 November 2021

For more information, contact us at: ICEAINT@univ-oeb.dz

Website address : http://www.univ-oeb.dz/vrlex/en/2021/3717/

Paper Submission

Authors are invited to submit full-length papers (8 pages max) written in English, and formatted using the IEEE templates.

The papers should be submitted electronically in PDF format through the CMT platform:

https://cmt3.research.microsoft.com/ICEAINT2021

All papers will be double blind peer-reviewed. Acceptance will be based on quality, relevance, originality, and presentation. All papers submitted to the ICEAINT'21 must be previously unpublished

Torque Ripple Reduction of Induction Machine A Comparison between Two Approaches DTC-SVM

Lakhdar Djaghdali

Department of electrical Engineering, University of Msila, Algeria
djaghdali.lakhdar@univ-msila.dz

Abstract – The paper deals with a comparison between two DTC-SVM approaches: DSVM-DTC with a hysteresis controllers and MPDTC with a predictive controller. In DTC-SVM, the switching frequency is limited by the sampling frequency; its theoretical maximum value is half the sampling frequency. However, in reality the switching frequency is lower than this value, and thus, high flux and torque ripples occur compared with modulator-based control methods. In order to overcome this, an optimization problem is formulated and solved in real time. Thereby, apart from the regulation of the torque and the flux magnitude to their references, an additional control objective should be met: the minimization of the torque and flux ripple. To do so, the time point at which the switches of the inverter should change state is calculated. Following the formulation of both approaches, their implementation in the Matlab-Simulink environment has been treated. The transient behavior as well as the steady state features of the induction motor drive under both DTC-SVM approaches are compared and commented. The comparison is based on several criteria including: static and dynamic performance, structure and implementation complexity, and especially decoupling, torque and flux ripple. It has been found that the second approach MPDTC yields high dynamic performances in the whole speed range. These performances are characterized by a low torque ripple with a high capability to eliminate the demagnetization problem which penalizes the flux regulation at low speeds in the first DTC-SVM approach. However, the second DTC-SVM approach with a predictor controller requires much more CPU time than the first one.

Keywords - Induction motor, direct torque control, Predictive direct torque control, space vector modulation (SVM).

1. INTRODUCTION

Since direct torque control (DTC) was introduced in the mid-1980s by Takahashi and by Depenbrock, it has been widely used for induction machine drives [1], [2]. Besides its simplicity, DTC is able to produce fast torque and flux control. However, it is well known that DTC presents some disadvantages, such as the variable commutation frequency behavior of the inverter [3], and notable torque and flux ripples.

In recent years, many efforts have been made to improve the performance of DTC, especially by reducing the torque ripples and stator flux, and by fixing the inverter commutation frequency. Several studies investigated the possibility to associate space-vector modulation (SVM) techniques with DTC strategies in order to control the switching frequency [4], [5]. To overcome the aforementioned disadvantages for an IM drive, various methods have been presented in the literature. In [6] and [7], the matrix converter provides more voltage vectors modulation and hence, low torque and stator flux ripples can be achieved. However, in order to minimize these ripples and keep almost constant switching frequency, it is necessary to have an increasing number of power switches which lead to a reduced overall efficiency and a high cost. Second, the model predictive control (MPC) approach provides a possibility to determine the voltage vectors which result in the lowest torque and stator flux ripples [8]. However, this approach has the disadvantage that the control law complexity grows exponentially with the length of the prediction horizon. Third, the modified DTC scheme with a reference flux vector calculator (RFVC) for an IM drive is presented in [9], which achieves a good torque response regardless of the operating torque. However, the PWM switching frequency is relatively high compared to the other DTC approaches. Another modified method incorporates a space vector modulation (SVM) into the DTC structure. This DTC-SVM can regulate the torque and stator flux more accurately and moderately with fixed switching frequency. A variety of methods to calculate the voltage space vector reference have been presented in the literature [10]–[13]. As per author in [10], a discrete SVM technique with predefined switching instants and extended switching tables is described for the DTC strategy. Even if this scheme can operate with fixed switching frequency, it is only suitable for induction motor (IM) drives. In [11], the DTC-SVM including a proportional integral (PI) controller is presented to fulfill the reduced torque and flux ripple requirements. However, the torque and stator flux responses during low speed operations are not shown in detail. Also, the sliding mode control (SMC) method is suggested for the DTC-SVM of IM drives in [12]. Although this approach improves the static, dynamic, and sinusoidal tracking performances, and reduces the chattering of the sliding surface, only simulation results are provided as means of verification. In [14], the fuzzy control (FC) method for the DTC-SVM is presented to reduce the torque ripple. In this method, fast torque response and minimum torque ripples are the main advantages. However, many trials are required to properly select the membership function which guarantees the system stability. As mentioned above, each discussed method has its own benefits and limitations. In addition, the high nonlinearities of an IM have made it difficult to achieve the fast and stable control performance.

Recently, the nonlinear control technique based on the feedback linearization (FL) theory has been used for various applications in the area of power electronics and drives [15]. The main idea of the feedback linearization control (FLC) approach is to algebraically transform nonlinear system

dynamics into linear one so that linear control techniques can be applied. Furthermore, the control laws for nonlinear systems can be systematically established based on the FLC technique. These laws can be further verified in advance to accommodate the actual system model characteristics in real application. In [16] the adaptive neural fuzzy inference system method is based on fuzzy logic and artificial neural networks for decoupled stator flux and torque control. The stability will be affected by parameter variation and the system model must be known, as the system's dynamic performance and stability will be significantly affected by parameter variations.

Within these approaches, the paper devotes to a comparative study between the performances of two DTC-SVM: The comparison is based on several criteria including: static and dynamic performance, structure and implementation complexity, decoupling, torque and stator flux ripple.

This paper is organized in seven sections. The model of the induction machine is presented in the next section. The control method by DSVM – DTC and MPDTC will be discussed in section three and four. In the fifth and sixth sections, we present the technique of Space Vector Pulse Width Modulation (SVM) and we compare the simulation results. Finally, a general conclusion summarizes this work. The simulation results are obtained by using Matlab/Simulink.

2. MODEL OF THE INDUCTION MACHINE

Among the various types of models used to represent the induction machine, there is one that uses each of the stator currents, stator flux, and speed as state variables, voltages (V_{sd}, V_{sq}) as control variables. This model is presented in reference (d, q), related to the rotating field. This model is expressed by the following system of equations [17]:

$$\begin{cases} V_{ds} = R_s.I_{ds} + \frac{d\Phi_{ds}}{dt} - \omega_s.\Phi_{qs} \\ V_{qs} = R_s.I_{qs} + \frac{d\Phi_{qs}}{dt} + \omega_s.\Phi_{ds} \\ V_{dr} = 0 = R_r.I_{dr} + \frac{d\Phi_{dr}}{dt} - (\omega_s - p\Omega).\Phi_{qr} \\ V_{qr} = 0 = R_r.I_{qr} + \frac{d\Phi_{qr}}{dt} + (\omega_s - p\Omega).\Phi_{dr} \end{cases} \quad (1)$$

In addition, the components of the stator and rotor flux are expressed by:

$$\begin{cases} \Phi_{ds} = L_s.I_{ds} + L_m.I_{dr} \\ \Phi_{qs} = L_s.I_{qs} + L_m.I_{qr} \\ \Phi_{dr} = L_r.I_{dr} + L_m.I_{ds} \\ \Phi_{qr} = L_r.I_{qr} + L_m.I_{qs} \end{cases} \quad (2)$$

Moreover, the mechanical equation of the machine is given by :

$$j\frac{d\Omega}{dt} + f\Omega = T_e - T_r \quad (3)$$

The electromagnetic torque equation can be expressed in terms of stator currents and stator flux as follows:

$$T_e = P.(\Phi_{ds}.I_{qs} - \Phi_{qs}.I_{ds}) \quad (4)$$

3. DISCRETE SPACE VECTOR MODULATION FOR DIRECT TORQUE CONTROL DSVM-DTC

The command DSVM-DTC analyzes the problem of chattering introduced at the torque and flux in the classical DTC [18].The name DSVM stems from the fact that each sample period is divided into three equal time intervals so as to produce the technical Vector PWM. Thus, the voltage vectors number increase in an improvement of the trajectory of the flux vector and consequently a reduction of the corrugations. The control system uses predefined tables for each speed level complicating this approach [19].

3.1 Principle of command DSVM – DTC

3.1.1 Speed of the induced voltage

In this approach, there is an asymmetry in the behavior of the torque because of the induced voltage created by the speed under constant flux [19]. The DSVM calculates and uses this voltage to select a voltage vector. The range acceleration from Zero where the induced voltage is equal to the applied voltage vector is divided into three regions; low, medium and high.

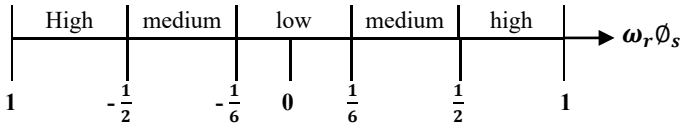

Figure 1. Voltage speed region [p.u]

The induced voltage is:

$\omega_r \begin{bmatrix} \emptyset_\alpha \\ \emptyset_\beta \end{bmatrix}$ its only value is the calculated voltage is used

$$\bar{V}_s = \omega_r \bar{\emptyset}_s \quad (5)$$

It is then compared to the regions.

3.1.2 Sector used in DSVM_DTC

The command DSVM_DTC uses twelve sectors instead of six; twelve sectors will be used for the high speed range. While the low and medium speed range only six sectors are used.

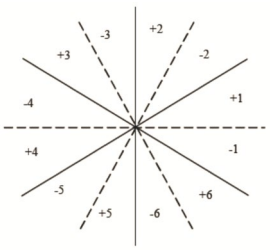

Figure 2. Sector of the ***DSVM- DTC***

3.1.3 Comparator hysteresis torque

The DSVM_DTC command can produce several voltage vectors if they are applied properly there will be less ripple in the torque and flux. To achieve this, one uses a hysteresis comparator to 5 levels instead of two for the torque.

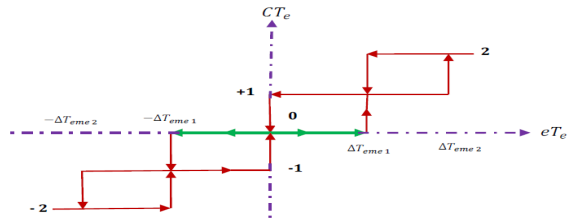

Figure 3. Torque hysteresis block

If the error of the torque is so small hysteresis is in state 0. In this case, a voltage vector is selected to maintain the torque at the current level. If hysteresis is capable +1 or - 1, the chosen vector must be means to hoist the couple in the small area. When hysteresis is capable +2 or - 2, the vector chosen to offset the error as soon as possible torque must be large enough, that is to say the same vector used in the conventional DTC.

3.1.4 Switching table

In this type of control the switching table has four input variables are the state of flux hysteresis, torque, sector number and the induced voltage by the speed (Figure 4). Since the command selects voltage vectors according to the induced voltage therefore each speed region using a corresponding switching table.

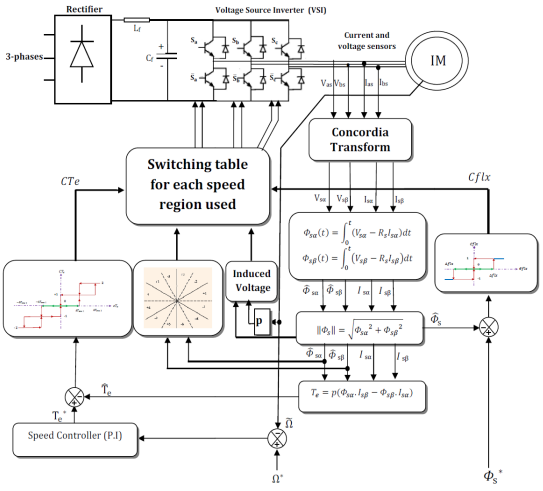

Figure 4. Block diagram of the general structure of the control **DSVM-DTC**

When the command runs in the high speed region two switching tables are used for each sector because of an asymmetry introduced by the induced voltage. Switching of the tables used in this case are also asymmetrical. For low and medium speed control one table is used for each sector. Thus different switching tables can be used depending on the direction of rotation.

3.1.5 Voltage inverter

In control DSVM_DTC each sample period is divided into three equal time intervals. In each interval is applied is an active vector is a zero vector. The inverter has to work three times the sampling frequency.
For example, U_{223} vector is synthesized by the application of U_{222} in the first two intervals, then U_{333}.

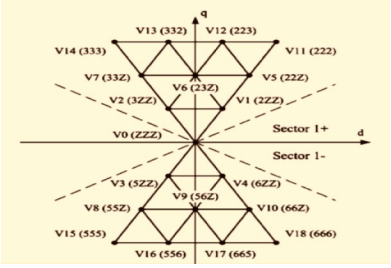

Figure 5. Vectors DSVM in sector (+ 1, -1)

3.1.6 Selecting tensions vectors

The induced voltage depends on the mechanical speed, when it increases; the voltage Vs applied to the machine also increases. The voltage vector $\overline{V}_s$ causes the flux $\overline{\emptyset}_s$ with an offset of $\frac{\pi}{2}$ so it is keyed on the axis $\beta^{\emptyset_s}$ the resulting vector that affects the couple is the component $V_\beta^{\emptyset_s}$ of the voltage vector delivered by the voltage inverter least $\overline{V}_s$ Therefore, the voltage vector V_s selection criterion is chosen as a reference. If $V_\beta^{\emptyset_s} \approx \overline{V}_s$ torque is maintained at its current state if $V_\beta^{\emptyset_s} > \overline{V}_s$ torque increases, and if $V_\beta^{\emptyset_s} < \overline{V}_s$ torque decreases.

a. Region at low speed

The voltage vector $\overline{V}_s$ is close to zero when it is in low-speed region. The switching vectors are chosen symmetrically around zero according to the low speed table. This switching table depends on the direction of motor rotation. If the estimated torque is close to the reference value, the hysteresis state of the torque is zero and therefore the voltage vector selected is zero. If the hysteresis torque state is +1 or -1, a moderate increase or decrease, respectively, is sought. The selection of the voltage vector is made between U_{200}, U_{300}, U_{500} and U_{600}. To increase the torque U_{200} and U_{600} stream must be chosen. While U_{300} and U_{500} are used to decrease the flux. When the gap between the reference torque and estimated is great that is to say CTe = +2 or -2, the command DSVM_DTC imposes an identical choice than the conventional DTC. Thus, U_{222} vectors U_{333}, U_{555} and U_{666} are selected to make up the gap as quickly as possible.

CTe / Cflx	-2	-1	0	1	2
-1	U_{555}	U_{500}	U_{000}	U_{300}	U_{333}
1	U_{666}	U_{600}	U_{000}	U_{200}	U_{222}

Table 1. Switching table for low positive speed, sector (+1,-1).

b. Region at medium speed

In the region of medium speed $V_n / 6 < |V_s| < V_n / 2$ the induced voltage begins to introduce an asymmetry in the behavior of the torque. For positive V_s and CTe = 0, the control DSVM_DTC considers the choice of U_{200} and U_{300},

since these vectors make $V_{\beta}^{\emptyset s}$ approximately equal to V_s while maintaining torque at its current level. The choice of the U_{200} imposes an increased flux while U_{300} allows a reduction of the flux. For CTe = -1 a slight decrease in torque, the voltage vector is selected U_{000}, because it is the only vector at this level can be chosen for the two cases of the gap of flux. For CTe = +1, U_{220} is selected when the flux should be increased and U_{330} when one wants a decrease. When CTe = 2 or - 2, the control DSVM_DTC exploits the principle of the conventional DTC control.

CTe / Cflx	-2	-1	0	1	2
-1	U_{555}	U_{000}	U_{300}	U_{330}	U_{333}
1	U_{666}	U_{000}	U_{200}	U_{220}	U_{222}

Table 2. Switching table for positive average speed, sector (+1,-1).

c. *Region at High speed*

In the high speed region,$|V_s| > V_n / 2$, each sector is divided into two and all available vectors are used. Thus, the induced voltage is reduced considerably. Suppose $\emptyset_s$ is in the sector -1 and if the torque is to be kept at zero, the U_{220} and U_{230} voltage vectors are selected based on the reference flux. To reduce torque (CTe = -1), the choice of the closest and lower tensions vectors $V_{\beta}^{\emptyset s}$ are U_{200} or U_{300}. To increase torque (CTe = 1), there are two possibilities, either the increase in the flux with the selection of tensions vectors U_{222} and U_{223}, or decreasing the flux with the choice of tension vectors U_{332} and U_{333}. When switching the error of torque from zero to one, we notice that there are several switches of the voltage vector in the switching tables thus reducing ripples in the stream (U_{230}, U_{220}, U_{332}, U_{222} for the sector-1). In the case where the hysteresis comparator of the torque CTe = + 2 or -2, the selected voltage vectors are maximum and identical to those of the medium and low speed.

CTe / Cflx	-2	-1	0	1	2
-1	U_{555}	U_{300}	U_{230}	U_{332}	U_{333}
1	U_{666}	U_{200}	U_{220}	U_{222}	U_{222}

Table 3. Switching table for high positive speed, sector -1.

CTe / Cflx	-2	-1	0	1	2
-1	U_{555}	U_{300}	U_{330}	U_{333}	U_{333}
1	U_{666}	U_{200}	U_{230}	U_{223}	U_{222}

Table 4. Switching table for high positive speed, sector +1.

4. PREDICTIVE DIRECT TORQUE CONTROL (MPDTC)

The Predictive control is a technique of advanced control automation. It aims to control complex industrial systems [20]. The basic principle of predictive control is taken into account, at the current time, the future behavior, through explicit use of a numerical model of the system in order to predict the output in the future, on a finite horizon [21].One of the advantages of predictive methods lies in the fact that for a pre-calculated set on a horizon, it is possible to exploit the information of predefined trajectories located in the future, given that the aim is to match the output of system with this set on a finite horizon [21] (figure.6).

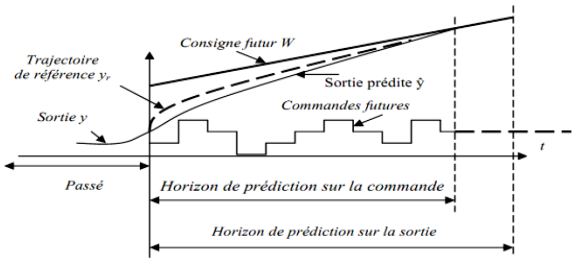

Figure.6 Time evolution of the finite horizon prediction

4.1 Formulation of The Model

All algorithms predictive control differs from each other by the model used to represent the process and the cost function to be minimized [23]. We will give for our formulation, the technique of the linearization input-output of the induction machine, in order to give a linearized model; module of the stator flux and the torque are uncoupled. The interest of such approach is to linearize the model of the machine and to obtain a homogeneous behavior whatever the point of operation.

We recall the system of the equations of the induction machine in the reference (α, β) which is given by:

$$\begin{cases} \frac{dI_{s\alpha}}{dt} = -\left(\frac{R_s}{\sigma L_s} + \frac{R_r}{\sigma L_r}\right) I_{s\alpha} - \omega_r I_{s\beta} + \frac{R_r}{\sigma L_r L_s}\phi_{s\alpha} + \frac{\omega_r}{\sigma L_s}\phi_{s\beta} + \frac{1}{\sigma L_s} V_{s\alpha} \\ \frac{dI_{s\beta}}{dt} = -\left(\frac{R_s}{\sigma L_s} + \frac{R_r}{\sigma L_r}\right) I_{s\beta} + \omega_r I_{s\alpha} + \frac{R_r}{\sigma L_r L_s}\phi_{s\beta} - \frac{\omega_r}{\sigma L_s}\phi_{s\alpha} + \frac{1}{\sigma L_s} V_{s\beta} \\ \frac{d\phi_{s\alpha}}{dt} = V_{s\alpha} - R_s I_{s\alpha} \\ \frac{d\phi_{s\beta}}{dt} = V_{s\beta} - R_s I_{s\beta} \end{cases}$$

… (6)

The generated torque can be expressed in terms of stator currents and stator flux as follows:

$$T_e = p\left(\phi_{s\alpha} I_{s\beta} - \phi_{s\beta} I_{s\alpha}\right) \quad (7)$$

The system of equations receives in the form suggested for the application of the linearization within the meaning of the input-output as follows:

$$\begin{cases} \dot{x} = f(x) + g_1(x) V_{s\alpha} + g_2(x) V_{s\beta} \\ y = h(x) \end{cases} \quad (8)$$

With:

$$f(x) = \begin{bmatrix} f_1(x) \\ f_2(x) \\ f_3(x) \\ f_4(x) \end{bmatrix} =$$

$$\begin{bmatrix} -\left(\frac{R_s}{\sigma L_s}+\frac{R_r}{\sigma L_r}\right) I_{s\alpha} - \omega_r I_{s\beta} + \frac{R_r}{\sigma L_r L_S}\phi_{s\alpha} + \frac{\omega_r}{\sigma L_S}\phi_{s\beta} \\ -\left(\frac{R_s}{\sigma L_s}+\frac{R_r}{\sigma L_r}\right) I_{s\beta} + \omega_r I_{s\alpha} + \frac{R_r}{\sigma L_r L_S}\phi_{s\beta} - \frac{\omega_r}{\sigma L_S}\phi_{s\alpha} \\ -R_s I_{s\alpha} \\ -R_s I_{s\beta} \end{bmatrix} \quad (9)$$

Where the vector of states x and the commands u are:

$$x = \left[I_{s\alpha}, I_{s\beta}, \phi_{s\alpha}, \phi_{s\beta}\right]^t, \quad u = [V_{s\alpha}, V_{s\beta}]^t$$

And: $g_1(x) = \left[\frac{1}{\sigma L_s}, 0, 1, 0\right]^t$, $g_2(x) = \left[0, \frac{1}{\sigma L_s}, 0, 1\right]^t$

4.2.1 Control Flux-Torque:

Our concern is to minimize the pulsations of the torque and the flux of the induction machine. For that, we chose the torque and the module of stator flux like variables to be controlled; thus the vector of output is given by the equation according to:

$$y = \begin{bmatrix} h_1 \\ h_2 \end{bmatrix} = \begin{bmatrix} T_e \\ |\emptyset_s|^2 \end{bmatrix} = \begin{bmatrix} p\left(\phi_{s\alpha} I_{s\beta} - \phi_{s\beta} I_{s\alpha}\right) \\ \phi_{s\alpha}^2 + \phi_{s\beta}^2 \end{bmatrix} \quad (10)$$

4.2.2 Input-Output Linearization:

The method of the input-output linearization is developed starting from the theories of the differential geometry [24]. It consists of using the derivative of Dregs to express the model of the machine in relation to input-output. To obtain the non-linear law of control, let us derive as much from time than it is necessary in order to reveal the entry u. The derivatives of the two outputs are given by:

$$\begin{aligned} \dot{y}_1 &= L_f h_1(x) + L_{g1} h_1(x) V_{s\alpha} + L_{g2} h_1(x) V_{s\beta} \\ &= \sum_{i=1}^{4} \frac{\partial h_1}{\partial x_i} f_i(x) + \sum_{i=1}^{4} \frac{\partial h_1}{\partial x_i} g_1(x) V_{s\alpha} + \\ &\quad \sum_{i=1}^{4} \frac{\partial h_1}{\partial x_i} g_2(x) V_{s\beta} \end{aligned} \quad (11)$$

With:

$$\begin{aligned} \boldsymbol{L_f h_1} &= -p\phi_{s\beta}\left[-\left(\frac{R_s}{\sigma L_s}+\frac{R_r}{\sigma L_r}\right) I_{s\alpha} - \omega_r I_{s\beta} + \frac{R_r}{\sigma L_r L_S}\phi_{s\alpha} + \frac{\omega_r}{\sigma L_S}\phi_{s\beta}\right] \\ &\quad + p\phi_{s\alpha}\left[-\left(\frac{R_s}{\sigma L_s}+\frac{R_r}{\sigma L_r}\right) I_{s\beta} + \omega_r I_{s\alpha} + \frac{R_r}{\sigma L_r L_S}\phi_{s\beta} - \frac{\omega_r}{\sigma L_S}\phi_{s\alpha}\right] \\ \boldsymbol{L_{g1} h_1} &= p\left(I_{s\beta} - \frac{1}{\sigma L_s}\phi_{s\beta}\right) \\ \boldsymbol{L_{g2} h_1} &= p\left(\frac{1}{\sigma L_s}\phi_{s\alpha} - I_{s\alpha}\right) \end{aligned} \quad (12)$$

$$\begin{aligned} \dot{y}_2 &= L_f h_2(x) + L_{g1} h_2(x) V_{s\alpha} + L_{g2} h_2(x) V_{s\beta} \\ &= \sum_{i=1}^{4} \frac{\partial h_2}{\partial x_i} f_i(x) + \sum_{i=1}^{4} \frac{\partial h_2}{\partial x_i} g_1(x) V_{s\alpha} + \\ &\quad \sum_{i=1}^{4} \frac{\partial h_2}{\partial x_i} g_2(x) V_{s\beta} \end{aligned} \quad (13)$$

With:

$$\begin{cases} \boldsymbol{L_f h_2} = -2R_s\left(\phi_{s\alpha} I_{s\alpha} - \phi_{s\beta} I_{s\beta}\right) \\ \boldsymbol{L_{g1} h_2} = 2\phi_{s\alpha} \\ \boldsymbol{L_{g2} h_2} = 2\phi_{s\beta} \end{cases} \quad (14)$$

4.2.3 Linearization of the System:

The matrix defining the relation between the inputs of the system and its derived outputs is given by the expression:

$$\begin{bmatrix} \dot{y}_1 \\ \dot{y}_2 \end{bmatrix} = A(x) + D(x) \begin{bmatrix} V_{S\alpha} \\ V_{S\beta} \end{bmatrix} \quad (15)$$

With: $A(x) = \begin{bmatrix} L_f h_1 \\ L_f h_2 \end{bmatrix}$;

$$D(x) = \begin{bmatrix} L_{g1} h_1 & L_{g2} h_1 \\ L_{g1} h_2 & L_{g2} h_2 \end{bmatrix}$$

$$= \begin{bmatrix} p\left(I_{s\beta} - \frac{1}{\sigma L_s}\phi_{s\beta}\right) & p\left(\frac{1}{\sigma L_s}\phi_{s\alpha} - I_{s\alpha}\right) \\ 2\phi_{s\alpha} & 2\phi_{s\beta} \end{bmatrix}$$

$D(x)$: Is decoupling Matrix.

$$\begin{aligned} \text{Det}[D(x)] &= p\left(I_{s\beta} - \frac{1}{\sigma L_s}\phi_{s\beta}\right).2\phi_{s\beta} - \\ &\quad p\left(\frac{1}{\sigma L_s}\phi_{s\alpha} - I_{s\alpha}\right).2\phi_{s\alpha} \end{aligned} \quad (16)$$

After simplification, we get:

$$\begin{aligned} \det[D(x)] &= 2p\left[\frac{-1}{\sigma L_s}\left(\phi_{s\beta}{}^2 + \phi_{s\alpha}{}^2\right) + I_{s\beta}\phi_{s\beta} + \right. \\ &\quad \left. I_{s\alpha}\phi_{s\alpha}\right] \neq \mathbf{0} \end{aligned} \quad (17)$$

The determinant of the matrix D(x)is different from zero; therefore D(x)is a reversible matrix.

$$D^{-1}(x) = \frac{1}{2p\left[\frac{-1}{\sigma L_s}\left(\phi_{s\beta}{}^2 + \phi_{s\alpha}{}^2\right) + I_{s\beta}\phi_{s\beta} + I_{s\alpha}\phi_{s\alpha}\right]} \begin{bmatrix} 2\phi_{s\beta} & -p\left(\frac{1}{\sigma L_s}\phi_{s\alpha} - I_{s\alpha}\right) \\ -2\phi_{s\alpha} & p\left(I_{s\beta} - \frac{1}{\sigma L_s}\phi_{s\beta}\right) \end{bmatrix} \quad \text{... (18)}$$

The linearization following input-output which is introduced for the system illustrated by (l'eq-8) is given by:

$$\begin{bmatrix} V_{s\alpha} \\ V_{s\beta} \end{bmatrix} = D^{-1}(x)\left[-A(x) + \begin{bmatrix} V_1 \\ V_2 \end{bmatrix}\right] \quad (19)$$

$V = \begin{bmatrix} V_1 \\ V_2 \end{bmatrix}$: represent the new vector of input.

The application of the law linearizing (l'eq-19) on the system (l'eq-15) led to two linear and uncoupled mono variable system:

$$\begin{cases} V_1 = \dot{h_1}(x) \\ V_2 = \dot{h_2}(x) \end{cases} \quad (20)$$

To ensure perfect regulation and track the desired signals of the flux and torque toward their reference, V_1 and V_2 are chosen as follows:

$$\begin{cases} V_1 = \left|\dot{\emptyset}_s\right|_{ref}^2 + k_1\left(|\emptyset_s|_{ref}^2 - |\emptyset_s|^2\right) \\ V_2 = \dot{T}_{e\,ref} + k_2\left(T_{e\,ref} - T_e\right) \end{cases} \quad (21)$$

Here, the subscript 'ref' denotes the reference value and (k_1, k_2) are constant design parameters to be determined in order to make the decoupled system in (Eq. 15) stable. The behavior of the linearized model is imposed by the pole placement method. The coefficients selected, such as $s + k_1$ and $s + k_2$, are the Hurwitz polynomials [25].

4.3 Criterion of Optimization:

We must find the future control sequence to apply on the system to reach the desired set point by following the reference trajectory. To do this, we just minimize a cost function which differs according to the methods, but generally this function contains the squared errors between the reference trajectory and the predictions of the prediction horizon and the variation of the control [21] [22]. This cost function is given as follows:

$$J = \sum_{j=N_1}^{N_2} [w(t+j) - \hat{y}(t+j)]^2 + \lambda \sum_{j=1}^{N_u} \Delta u(t+j-1)^2$$

…(22)

With:

w (t + j): Set point applied at time (t + j).

$\hat{y}(t+j)$: Output predicted time (t + j). Δu (t + j-1): Increment of control at the moment (t + j-1).

N_1: Minimum prediction horizon on the output.

N_2: Maximum prediction horizon on the output, with $N_2 \geq N_1$.

N_u : Horizon prediction on the order.

λ: Weighting factor on the order.

T_s: The period of sampling.

The definition of the quadratic criterion showed that the user must set four parameters. The choice of parameters is difficult because there is no empirical relationship to relate these parameters to conventional measures automatically.

The model linearized and uncoupled from the induction machine, so that it is established inside the predictive control, which is shown by (Figure. 7).

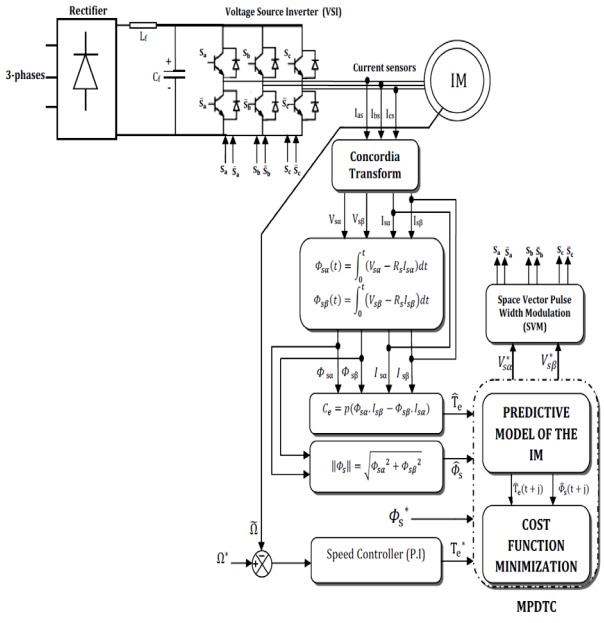

Figure 7. Diagram block of the predictive direct torque control

5. Space Vector Pulse Width Modulation

The SVM technique was first presented by a group of German researched in the second half of the 1980s [26]. Since then, a lot of work has been done on the theory and implementation of SVM techniques. SVM techniques have several advantages that are offering better DC bus utilization, lower torque ripple, lower Total Harmonic Distortion (THD) in the AC motor current, lower switching losses, and easier to implement in the digital systems. At each cycle period, a preview technique is used to obtain the voltage space vector required to exactly compensate the flux and torque errors. The torque ripple for this SVM-DTC is significantly improved and switching frequency is maintained constant. The voltage vectors, produced by a 3-phase PWM inverter, divide the space vector plane into six Sectors as shown in Figure (8.A).

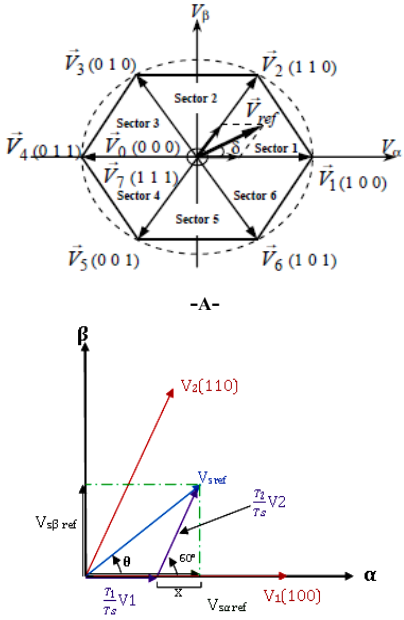

-A-

-B-

Figure 8. Switching States of SVM .Projection of the Reference Voltage Vector

SVM, based on the switching between two adjacent boundary active vectors and a zero vector during one switching period T_s, and for a given reference voltage vector in the first sector $(0 - \frac{\pi}{3})$ is shown in Figure (8.B). $\overline{V}_{s\,ref}$ is a synthesized voltage, space vector and its equation is given by:

$$\bar{V}_{s\,ref} T_s = \bar{V}_0 T_0 + \bar{V}_1 T_1 + \bar{V}_2 T_2 \quad (23)$$

$$T_s = T_0 + T_1 + T_2 \quad (24)$$

Where, T_0 , T_1 and T_2 is the work time of basic space voltage vectors $\overline{V}_0$, $\overline{V}_1$ and $\overline{V}_2$.

The determination of the Amount of times T_1 and T_2 given by mere projections is:

$$\begin{cases} V_{s\alpha\,ref} = \frac{T_1}{T_S}|\bar{V}_1| + x \\ V_{s\beta\,ref} = \frac{T_2}{T_S}|\bar{V}_2| \sin\left(\frac{\pi}{3}\right) \\ x = \frac{V_{s\beta\,ref}}{\mathrm{tg}(\frac{\pi}{3})} \end{cases} \Rightarrow$$

$$\begin{cases} T_1 = \frac{T_S}{2U_{dc}}\left(\sqrt{6}V_{s\alpha\,ref} - \sqrt{2}V_{s\beta\,ref}\right) \\ T_2 = \frac{T_S\sqrt{2}}{U_{dc}} V_{s\beta\,ref} \end{cases} \quad (25)$$

6. THE RESULTS OF SIMULATIONS

In this section, the effectiveness of the second approach for torque and flux control of an IM is verified by computer simulations. A series of tests were conducted to check the performance of the proposed system.

6.1 Influence Horizon of Prediction N_2

N_2 is varied to see its effect on performance. The following figures show the evolution of the output (torque and stator flux) for different values of N_2.

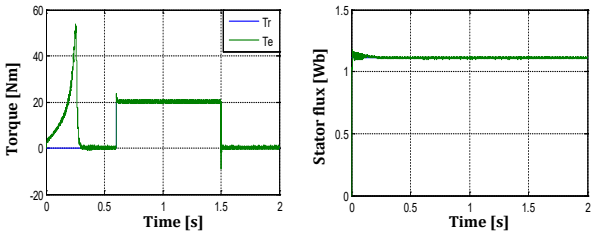

Figure.9 Evolution of the torque and stator flux magnitude for: N_1=1, **N_2=20**, N_u=1, λ=0.8, T_s=0.00001s.

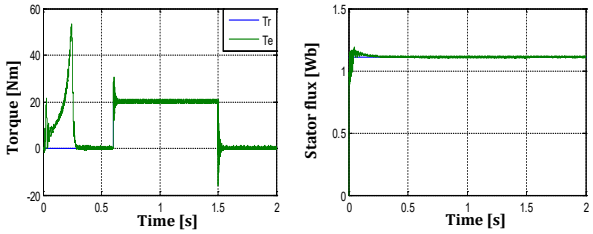

Figure.10 Evolution of the torque and stator flux magnitude for: N_1=1, **N_2=10**, N_u=1, λ=0.8, T_s=0.00001s.

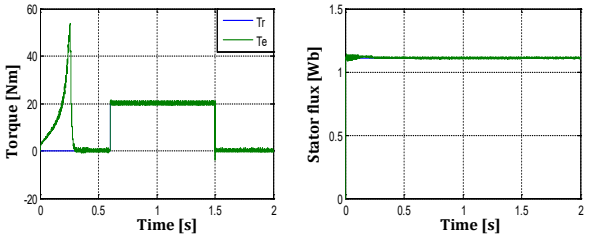

Figure.11 Evolution of the torque and stator flux magnitude for: N_1=1, **N_2=30**, N_u=1, λ=0.8, T_s=0.00001s.

6.2 Influence Weighting Coefficient λ

λ is varied to see its effect on performance. The following figures show the evolution of the output (torque and stator flux) for deferent values of λ:

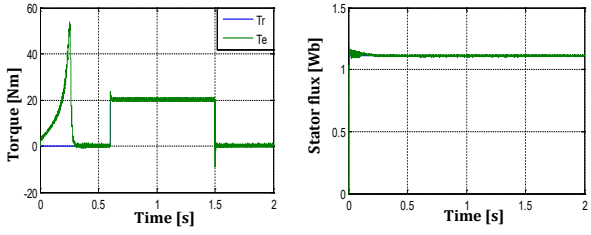

Figure.12 Evolution of the torque and stator flux magnitude for: N_1=1, N_2=20, N_u=1, **λ=0.8**, T_s=0.00001s.

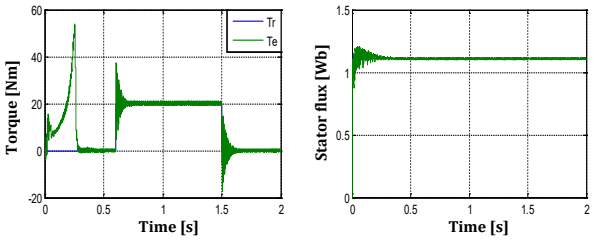

Figure. 13 Evolution of the torque and stator flux magnitude for**:** N_1=1, N_2=20, N_u=1, **λ=0.6**,T_s=0.00001s.

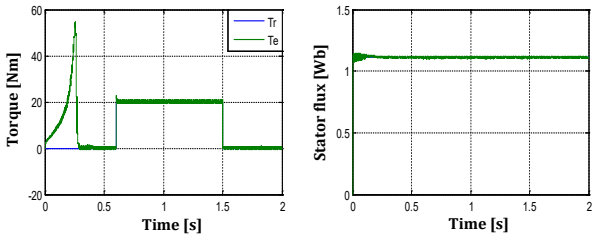

Figure. 14 Evolution of the torque and stator flux magnitude for**:** N_1=1, N_2=20, N_u=1, **λ=0.95**,T_s=0.00001s.

According to the results of the evolution of the output variables, we note that an increase in λ results in a reduction in the response time of the system and a reduction results in a large overshoot of the set point. Thus, a strong N_2 increase results slowly in answer the system, whereas a reduction results in a large overshoot of the set point especially on the level of flux.

Previous simulations call for several comments:

- We noted that the major drawback of predictive control is that the performance is greatly influenced by the choice of the synthesis parameters N_1, N_2, N_u, and ***λ*** therefore, a judicious choice of these parameters is necessary before the implementation of the simulation algorithm, to meet the desired performance.
- When there are actually values of the set point in the future, all of these informations are used between horizons of N_1 and N_2 so as to converge the predicted output to this set point.
- The coefficient λ is used to give more or less weight to the control relative to the output, so as to ensure the convergence when the starting system is a risk of instability.

6.3 Comparisons of simulations

In what follows, we consider the transient behavior of the induction motor under a reference speed. The results of two approaches are shown in Figures 15, 16 and 17.

Referring to figures (16) shows the speed response of MPDTC and DSVM-DTC controller. The MPDTC reacts faster than the DSVM-DTC when load torque is suddenly applied and removed.

Moreover, tracking performances were improved by the use of the MPDTC law, in comparison with those of DSVM-DTC. These properties make the new algorithm suitable for applications where high tracking accuracy is required in the presence of external disturbances.

Comparing figures (15), the second approach MPDTC

offers a notable reduction of the electromagnetic torque ripple compared to the first using hysteresis controllers.

Referring to figures (17) the magnitude of the stator flux is quickly established at its reference value, in both control techniques. The MPDTC has a visible reduction in oscillation amplitude of the modulus of the flux with respect to the DSVM-DTC. The dynamic component of the stator flux is not affected by the application of the load command. The MPDTC has as good of a dynamic response as the first approach.

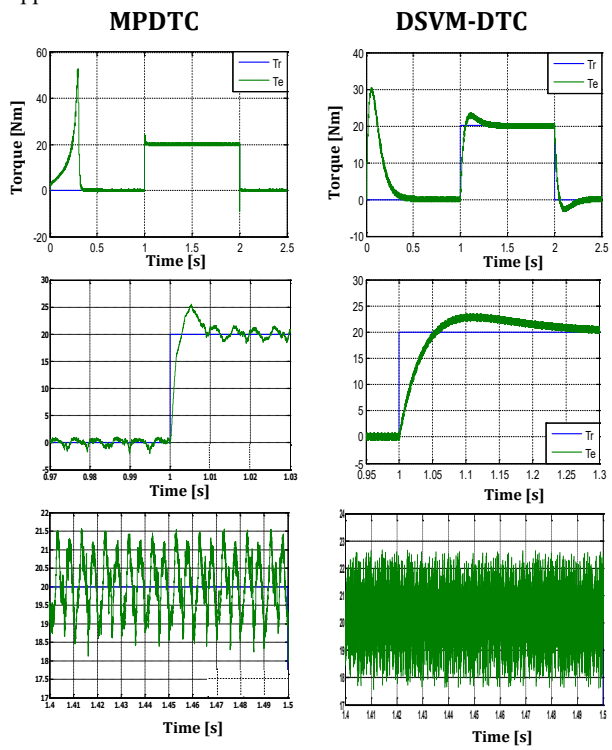

Figure.15 Comparison of the electromagnetic torque

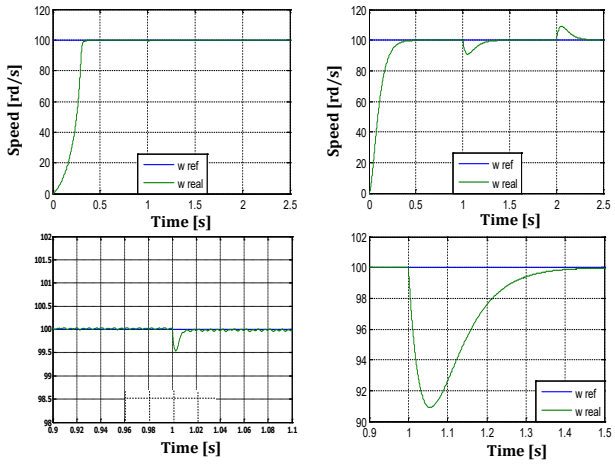

Figure. 16 Comparison the speed of rotation

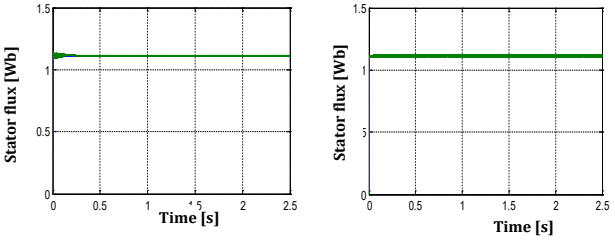

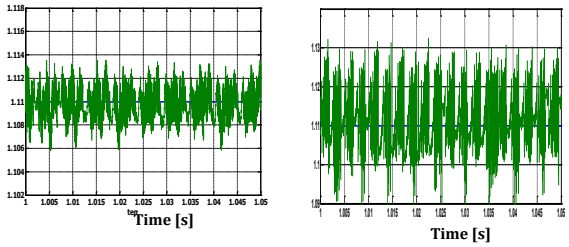

Figure.17 Comparison of the stator flux magnitude

(Table. 5) summarizes the results of the comparative study treated previously. In fact from this table, one can choose the approach to be used according to the needed objectives, the desired performances and the available means.

Control Approach	DSVM-DTC	MPDTC
Electromagnetic torque ripples	high	low
Stator flux ripples	high	low
Switching losses	high	low
rejection of disturbance	Bad	good
Algorithm complexity	medium	high
Commutation frequency	fixed	fixed
computing time	medium	high

Table 5. Comparison between Performances of the two DTC-SVM Approaches

Characteristics of the machine used for simulation:

parameter	*symbol*	*Value*
Number of pole pairs	p	2
Power	P_u	3 KW
Line voltage	U_n	380V
Line current	I_n	6.3A
Nominal frequency	f	50Hz
Mechanical rotor speed	N_n	1430 tr/mn
Electromagnetic torque	T_e	20Nm
Stator Resistance	R_s	3.36 Ω
Rotor Resistance	R_r	1.09 Ω
Stator cyclic inductance	L_s	0.256H
Mutual cyclic Inductance	L_m	0.236H
Rotor cyclic inductance	L_r	0.256H
Rotor inertia	j	$4{,}5.10^{-2}$Kg.m^2
Viscosity coefficient	f	$6{,}32.10^{-4}$N.m.s

7. CONCLUSION

This paper has been devoted to the comparison between the performance of the DSVM_DTC strategy with hysteresis controllers and those of a MPDTC with a predictive controller has been carried out considering simulation works. The transient behavior as well as the steady state features of the induction motor drive under both DTC-SVM approaches have been compared and commented. Simulation works have clearly shown that the second approach yields high dynamic performance in torque and

stator flux module with lower ripple, than the first one, as well as rejection disturbance at speed. However, the MPDTC with a predictive controller would inevitably require control systems with higher CPU frequencies in so far as their implementation schemes are more complicated than those of the first one.

REFERENCES

[1] I. Takahashi and T. Noguchi. A new quick-response and high-efficiency control strategy of an induction motor. IEEE Transaction industry Applications, IA-16: 820-827, Sept/Oct 1986.

[2] M.P. Kazmierkows and A.B. Kasprowicz. Improved direct torque and flux vector control of PWM inverter-fed induction motor drives. IEEE Transactions on industrial Electronics, 42(4): 344-350, August 1995.

[3] A. Yangui F. Ben Salem and A. Masmoudi. On the reduction of the commutation frequency in DTC : a comparative study. European Transactions on Electrical Power Engineering (ETEP), 15(6): 571-584, 2005.

[4] P. Chlebis P. Brandstetter and P. Palacky. Direct torque control of induction motor with direct calculation of voltage vector. Advances in Electrical and Computer Engineering Journal, 10(4): 17-22, 2010.

[5] A. Joseline Metilda R. Arunadevi, N. Ramesh and C. Sharmeela. Analysis of direct torque control using space vector modulation for three phase induction motor. Recent Research in Science and Technology, 3(7): 37-40, 2011.

[6] M. Borujeni, F.; Ardebili, M. "DTC-SVM control strategy for induction machine based on indirect matrix converter in flywheel energy storage system". Power Electronics, Drives Systems & Technologies Conference (PEDSTC), 2015 6th .Pages: 352 – 357.

[7] M. Farhad; Khaburi, D.A. " Torque ripple reduction in direct torque control of induction machines by use of all voltage vectors of matrix converters". Power Electronic & Drive Systems & Technologies Conference (PEDSTC), 2010 . Pages: 261 – 266.

[8] Y. Zhang ; H. Yang « Torque Ripple Reduction of Model Predictive Torque Control of Induction Motor Drives" Energy Conversion Congress and Exposition (ECCE), 2013. Pages: 1176 – 1183.

[9] Y. Inoue, S. Morimoto, and M. Sanada, "Examination and linearization of torque control system for direct torque controlled IPMSM," IEEE Trans. Ind. Appl., vol. 46, no. 1, pp. 159–166, Jan./Feb. 2010.

[10] C. Patel, R. P. P. A Day, A. Dey, R. Ramchand, K. Gopakumar, and M. P. Kazmierkowski. "Fast direct torque control of an open-end induction motor drive using 12-sided polygonal voltage space vectors," IEEE Trans. Power Electron., vol. 27, no. 1, pp. 400–410, Jan. 2012.

[11] Y. Kumsuwan. "Reduction of Torque Ripple In Direct Torque Control For Induction Motor Drives Using Decoupled Amplitude and Angle of Stator Flux Control". ECTI Trans On Electrical Eng, Electronics and Communication VOL 8, N° 2 august 2010. pp 187-196.

[12] D. Sun "Sliding Mode Direct Torque Control for Induction Motor with Robust Stator Flux Observer". Intelligent Computation Technology and Automation (ICICTA), 2010 International Conference, Year: 2010, Volume: 3, Pages: 348 – 351.

[13] S. Benaicha; F. Zidani; R.N. Said; M.S.N. Said. "A novel direct torque fuzzy control of SVM-inverter-fed induction motor drive". Power Engineering, Energy and Electrical Drives (POWERENG), 2013 Fourth International Conference. Year: 2013; Pages: 340 – 345.

[14] H. Li, Q. Mo, Z. Zhao. "Research on direct torque control of induction motor based on genetic algorithm and fuzzy adaptive PI controller", Measuring Technology and Mechatronics Automation, Vol. 3, pp. 46-49, 2010.

[15] W. Zhao, D. D. C. Lu, and V. G. Agelidis, "Current control of grid connected boost inverter with zero steady-state error," IEEE Trans. Power Electron., vol. 26, no. 10, pp. 2825–2834, Oct. 2011.

[16]T. Riad, B. Hocine, M. Salima, "New direct torque neuro-fuzzy control based SVM-three level inverter-fed induction motor", International Journal of Control, Automation, and Systems, Vol. 8, pp. 425-432, 2010.

[17] G. Grellet, G. Clerc, " Electric Actuators, Principle, Models, Order ". Electro Collection. Eyrolles Edition 2000.

[18] D. Casadei, G. Serra, and A. Tani. "Implementation of DTC algorithm for induction motors based on discrete space vector modulation". IEEE Trans. On Power Electronics, vol 15, N04, pp769-777, July 2001.

[19] Reddy, M.R.P.; Brahmaiah, B.; Reddy, T.B. "Discrete space vector modulation algorithm based vector controlled induction motor drives for reduced ripple". Power and Energy Systems Conference: Towards Sustainable Energy, 2014, Pages: 1 – 5.

[20] G. Papafotiou, J. Kley, K. G. Papadopoulos, P. Bohren, and M. Morari. "Model predictive direct torque control - part II: Implementation and experimental evaluation". IEEE Trans. Ind. Electron., 56(6):1906–1915, Jun. 2009.

[21] J. B. Rawlings and D. Q. Mayne. " Model predictive control: Theory and design ". Nob Hill Publ 2009.

[22] A. Zaki Diab , D. Kotin, V. Pankratov " Speed Control of Sensorless Induction Motor Drive Based On Model Predictive Control" XIV International Conference On Micro/Nanotechnologies And Electron Devices Edm. IEEE 2013.

[23] E.F. Camacho, C.Bordons, "Model Predictive Control", Springer-Verlag London, 2sd édition, 2003.

[24] A. Djermoune, P. Goureau. "Input-output decoupling of nonlinear control for an induction machine". Industrial Electronics, 1996. ISIE '96., Proceedings of the IEEE International Symposium Year: 1996, Volume: 2 Pages: 879 – 884.

[25] A. Isidori, Nonlinear Control Systems, 2nd ed., New York, Springer, 1989.

[26] L. Chen, K.L. Fang, and Z.F. Hu, "A scheme of fuzzy direct torque control for induction machine", Proceedings of the Fourth International Conference on Machine Learning and Cybernetics, Guangzhou, pp. 803-807, 2005.